ACS Chemical Neuroscience

Article

Gut microbiota dynamics in Parkinsonian mice

Emily Klann, Massimiliano S Tagliamonte, Maria Ukhanova, Volker Mai, and Vinata Vedam-Mai

ACS Chem. Neurosci., **Just Accepted Manuscript** • DOI: 10.1021/acschemneuro.0c00386 • Publication Date (Web): 17 Sep 2020

Just Accepted

is published by the American Chemical Society. 1155 Sixteenth Street N.W., Washington, DC 20036

AUTHOR INFORMATION PAGE

Title: Gut microbiota dynamics in Parkinsonian mice

Authors: Emily Klann, MPH[1,2], Massimiliano S. Tagliamonte, DVM, PhD[2,3], Maria Ukhanova, PhD[2], Volker Mai, MPH, PhD[2*], Vinata Vedam-Mai, PhD[4*]

Affiliations: [1]Department of Epidemiology, College of Public Health and Health Professions and College of Medicine, University of Florida; [2]Emerging Pathogens Institute, University of Florida; [3]Department of Pathology, Immunology, and Laboratory Medicine, University of Florida; [4]Department of Neurology, University of Florida

TITLE PAGE

Manuscript title/running title: Gut microbiota dynamics in Parkinsonian mice

Number of characters in title: 44

Number of words in abstract: 246

Number of words in manuscript: 3,459

Number of tables: 3

Number of figures: 3

ABSTRACT

Peripheral immunity is thought to be dysregulated in Parkinson's disease (PD) and may provide an avenue for novel immunotherapeutic interventions. Gut microbiota is a potential factor for modulating immunotherapy response. Considering the possibly complex role of the gut-brain axis in PD, we used a preclinical model to determine the effects of gut microbiota dynamics in mice receiving an immunotherapeutic intervention compared to controls. A total of 17 M83 heterozygous transgenic mice were used in this study. Mice in the treatment arm (N=10) received adoptive cellular therapy (ACT) by injection and control mice (N=7) were injected with saline at 8 weeks of age. All mice received peripheral α-syn fibrils to hasten parkinsonian symptoms via an intramuscular injection one week later (9 weeks of age; baseline). Fecal pellets were collected from all mice at three time points post injection (baseline, 6 weeks and 12 weeks). DNA from each stool sample was extracted, 16S rDNA amplified and sequenced, and analyzed using QIIME2 and RStudio. Differences in the relative abundance of bacterial taxa were observed over time between groups. No significant differences in alpha diversity were found between groups at any timepoint. UniFrac measures of phylogenetic distance between samples demonstrated distinct clustering between groups post-baseline (p=0.002). These differences suggest that the gut microbiome may be capable of influencing immunotherapy outcomes. Conclusively, we observed distinctly different microbiota dynamics in treated mice compared to those in the control group. These results suggest a correlation between the gut-brain axis, PD pathology, and immunotherapy.

Key words: Parkinson's disease, gut microbiome, gut-brain axis, adoptive cellular therapy, mouse model, alpha synuclein

Abbreviations: ACT – adoptive cellular therapy, PD – Parkinson's disease

INTRODUCTION

Parkinson's disease (PD) is the second most common neurodegenerative disorder following Alzheimer's disease, with an estimated prevalence of approximately 1% in individuals over the age of 60[1]. PD is characterized by several motor as well as non-motor symptoms attributable to the chronic degeneration of dopaminergic neurons within the substantia nigra, and related circuitry. Cardinal motor features of PD include rigidity, tremor at rest, postural instability, and bradykinesia [2], while non-motor symptoms commonly include loss of sense of smell, rapid eye movement sleep behavior disorder, mood disturbances, cognitive changes, fatigue, and gastrointestinal issues[2,3]. Interestingly, accumulating evidence suggests that the onset of non-motor symptoms, gastrointestinal complications in particular, can considerably precede motor symptoms and the diagnosis of PD[4]. This is noteworthy considering the wealth of existing research suggesting a bidirectional relationship, known as the microbiota-gut-brain axis, between the commensal bacteria in the gut and the brain. More recently, the possible role of the microbiota-gut-brain axis in the development and progression of PD has been of interest. Multiple studies have established the presence of distinct differences in gut microbiota composition between individuals with PD and non-PD controls[5–7]. Gut dysbiosis, or the alteration of the structure and function of the communities of microbiota within the gut capable of disrupting homeostasis, has been associated with both the presence and severity of PD in humans[8]. Although there is some heterogeneity among existing studies of gut microbiome and PD, according to a recent review, *Rikenellaceae*, *Verrucomicrobiaceae*, and *Akkermansiaceae* have been found to be more abundant and *Prevotellaceae* and *Lachnospiraceae* have been found to be less abundant in PD patients compared to non-PD controls[9]. Further, supplementation with beneficial microbiota has been shown to reduce PD-related symptoms[10]. Considering this, maintenance of a healthy core microbiome and inhibition of dysbiosis may be important factors to slow the clinical progression of PD.

Chronic neuronal degeneration responsible for the eventual onset of PD symptoms likely is due to the accumulation of misfolded alpha-synuclein (α-syn) proteins around the neuronal synapses[11]. Although these aggregates are primarily observed in the brains of individuals with PD, they have also been observed in peripheral locations such as the enteric nervous system (ENS). Recent studies demonstrate the ability for peripherally injected α-syn fibrils to induce CNS pathology in M83 transgenic mouse models of PD[12,13], thus lending further

support to the possible role of the microbiota-gut-brain axis and peripheral routes of neuroinvasion in this disease. A cascade of immune events, such as microglial activation and increased cytokine production, result in persistent neuroinflammation[14]. Endotoxins, bacterial lipopolysaccharides (LPS) that frequently originate from the gut, also contribute to a chronic immune response and systemic inflammation through the stimulation of inflammatory cytokines[15]. Recent evidence suggests that peripheral inflammation and immune activation are capable of exacerbating neuroinflammation in individuals with PD and that treatment with anti-inflammatory medications may exert a neuroprotective effect in this population[16]. Thus, it may be reasonable to consider certain microbiota profiles (those with a high abundance of bacteria capable of producing and translocating LPS across the gut barrier) to have a synergistic effect on neuroinflammation originating from a response to α-syn aggregations in individuals with PD.

Given the importance of peripheral immune response in PD, there exists a need to further elucidate the potential role of the gut microbiota in the efficacy of novel therapeutic interventions, such as adoptive cellular therapy (ACT). ACT has traditionally been used as an alternative tumor-specific treatment option for some cancers, an effective treatment for viral infections, and a method of immune system augmentation following hematopoietic stem cell transplantation. Generally, ACT can be classified into three different types according to the mechanism of action into promotion of tumor-specific and tumor-infiltration lymphocytes, T lymphocyte receptor gene therapy, and chimeric antigen receptor modified T lymphocytes. Although ACT in the context of PD is still in its infancy, it may prove to be a promising therapeutic option if T lymphocytes can be modified to target abnormal α-syn during the early stages of disease pathology. In this study, we aimed to determine gut microbiota dynamics after peripheral `α-syn fibril injection` in the context of ACT treatment in M83 transgenic mice. We hypothesized that administration of ACT would be associated with underlying changes in the gut microbiota over time, which could potentially mediate overall therapeutic benefit in this disease model of PD.

RESULTS

A total of 57 fecal pellet samples from 17 mice were analyzed. We generated a total of 1,340,271 sequence reads with an average of 23,514 total reads per sample. A total of 1,115 unique OTUs were identified and included in all downstream analyses. These OTUs were classified into 8 phyla, 38 families, and 47 genera.

Dynamics in relative abundance of taxa over time

A total of 8 phyla were identified that were present in both the control and ACT groups across all time points. These included Actinobacteria, Bacteroidetes, Cyanobacteria, Deferribacteres, Firmicutes, Proteobacteria, Tenericutes, and TM7 (Table 1a and Figure 1). The most dominant phyla with the highest average relative abundance across all time points in ACT and controls were Bacteroidetes (54.5 and 59.3%), Firmicutes (39.2 and 37.3%), and Proteobacteria (1.6 and. 1.1%). A total of 16 families had an average relative abundance over 1% in at least one group and were consistently observed across all time points (Table 2a). The most dominant families with the highest average relative abundance across all time points in ACT and controls were *S24-7 (*family within the order Bacteroidales) (42.0 and 37.1%), *Lactobacillaceae* (19.8 and 18.7%), *Bacteroidaceae* (4.4 and 9.1%), *Ruminococcaceae* (4.1 and 5.1%), *Prevotellaceae* (2.7 and 3.2%), and *Rikenellaceae* (2.7 and 2.5%). Similarly, 11 genera with an average relative abundance over 1% in at least one group were observed consistently over time (Table 3a). The most dominant of these genera with the highest average relative abundance over time in the ACT

Figure 1. Relative abundance of phyla over time in the ACT and control groups

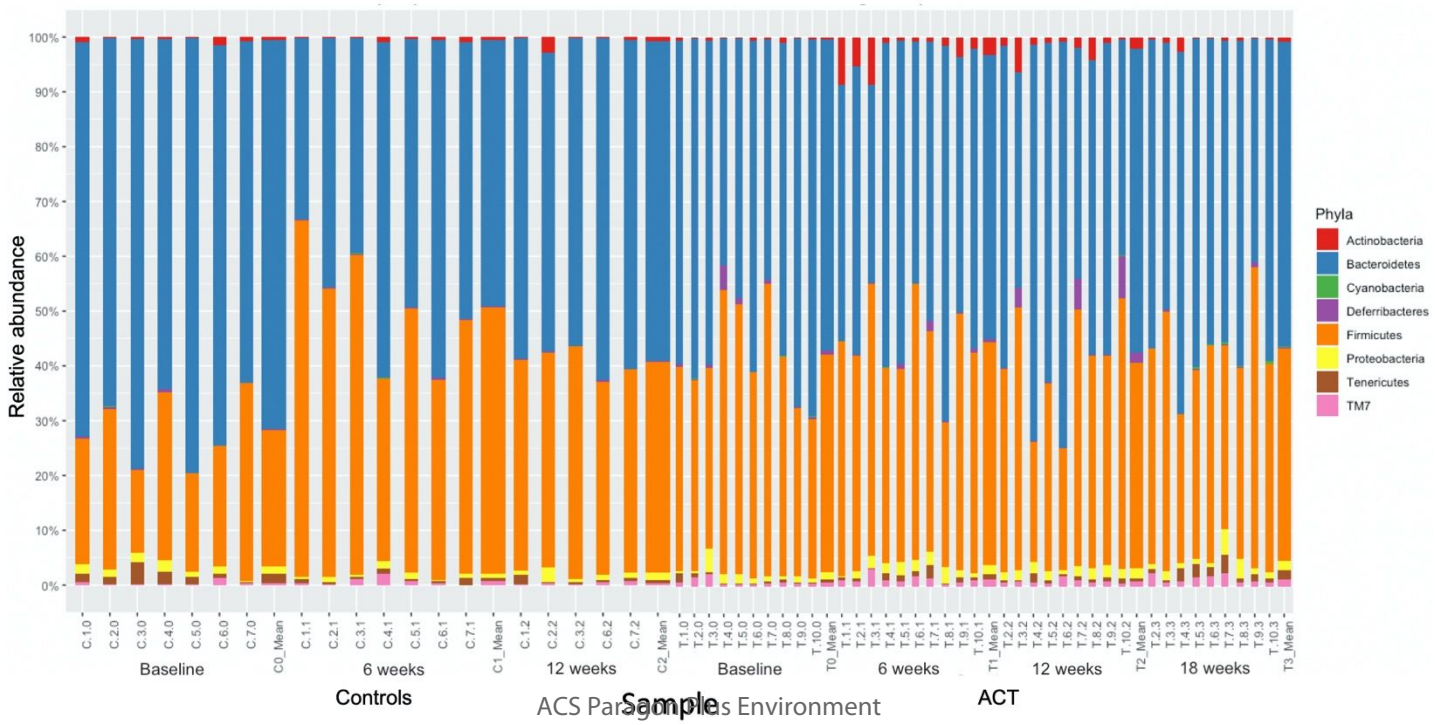

Relative abundance of phyla over time in the control and treatment (ACT) groups. Each bar represents an individual mouse. The average relative abundance for each time point within each group is shown as a bar with larger width.

and control groups include *Lactobacillus* (20.5 and 18.7%), *Bacteroides* (4.5 and 9.1%), *Oscillospira* (2.4 and 3.1%), and *Allobaculum* (1.2 and 3.3%).

Table 1a. Average relative abundance of phyla from time 0 to time 2 between control and treatment groups

	Time 0		Time 1		Time 2				
Phylum	**Control**	**ACT**	**Control**	**ACT**	**Control**	**ACT**	**T0 P-value†**	**T1 P-value†**	**T2 P-value†**
Actinobacteria	0.006	0.005	0.005	0.033	0.008	0.020	0.845	**0.042**	0.270
Bacteroidetes	0.709	0.565	0.486	0.518	0.583	0.553	**0.016**	0.601	0.699
Cyanobacteria	0.000	0.001	0.000	0.000	0.000	0.000	0.918	0.725	0.837
Deferribacteres	0.002	0.008	0.002	0.004	0.001	0.020	0.229	0.696	0.632
Firmicutes	0.249	0.396	0.486	0.406	0.385	0.374	**0.019**	0.435	0.898
Proteobacteria	0.013	0.013	0.008	0.018	0.013	0.018	0.788	0.061	0.546
Tenericutes	0.017	0.004	0.006	0.009	0.006	0.007	0.058	0.712	0.630
TM7	0.004	0.007	0.007	0.012	0.004	0.008	0.127	0.435	0.270
Unclassified	0.000	0.000	0.000	0.000	0.000	0.000	NA	0.462	0.325

Table 1b. Percent difference in relative abundance of phyla from time 0 to time 2 between control and treatment groups

	Time 0		Time 1		Time 2	
Phylum	**Difference (%)***	**T0 P-value†**	**Difference (%)***	**T1 P-value†**	**Difference (%)***	**T2 P-value†**
Actinobacteria	21.728	0.845	-148.932	**0.042**	-90.651	0.270
Bacteroidetes	22.604	**0.016**	-6.339	0.601	5.294	0.699
Cyanobacteria	-70.968	0.918	12.598	0.725	-25.806	0.837
Deferribacteres	-122.851	0.229	-80.381	0.696	-173.418	0.632
Firmicutes	-45.710	**0.019**	17.969	0.435	2.890	0.898
Proteobacteria	0.447	0.788	-81.141	0.061	-33.424	0.546
Tenericutes	117.737	0.058	-33.444	0.712	-15.909	0.630
TM7	-63.066	0.127	-50.481	0.435	-62.833	0.270

*Positive values indicate a higher relative abundance in the control group and negative values indicate a higher relative abundance in the ACT group. Percent difference calculated as: (average relative abundance in controls – average relative abundance in ACT)/[(average relative abundance in controls + average relative abundance in ACT)/2]

†Bolded values indicate statistical significance ($p<0.05$). P-values were generated with unpaired Mann-Whitney U tests and adjusted using the Benjamini-Hochberg method.

Table 2a. Average relative abundance of families from time 0 to time 2 between control and treatment groups

	Time 0		Time 1		Time 2				
Family	**Control**	**ACT**	**Control**	**ACT**	**Control**	**ACT**	**T0 P-value†**	**T1 P-value†**	**T2 P-value†**
[Odoribacteraceae]	0.039	0.009	0.008	0.011	0.006	0.012	0.168	0.139	0.753

Bacteroidaceae	0.130	0.053	0.068	0.041	0.076	0.038	**0.027**	0.370	0.596
Bifidobacteriaceae	0.002	0.002	0.001	0.017	0.005	0.016	0.673	0.572	0.276
Clostridiaceae	0.004	0.002	0.001	0.008	0.001	0.009	0.295	0.393	0.311
Defferribacteraceae	0.002	0.008	0.002	0.018	0.001	0.020	0.519	0.715	0.958
Erysipelotrichaceae	0.017	0.004	0.009	0.029	0.012	0.026	0.673	0.250	0.592
F16	0.004	0.007	0.007	0.008	0.004	0.008	0.377	0.321	0.223
Helicobacteraceae	0.004	0.004	0.004	0.009	0.005	0.011	0.584	0.265	0.592
Lachnospiraceae	0.021	0.043	0.030	0.019	0.026	0.021	**0.047**	0.600	0.276
Lactobacillaceae	0.061	0.121	0.303	0.236	0.197	0.236	0.470	0.299	0.592
Mycoplasmataceae	0.014	0.002	0.001	0.000	0.001	0.000	**0.045**	0.687	0.276
Porphyromonadaceae	0.031	0.006	0.007	0.007	0.011	0.005	**0.045**	0.606	0.383
Prevotellaceae	0.040	0.027	0.027	0.028	0.029	0.026	0.525	0.687	0.912
Rikenellaceae	0.029	0.018	0.024	0.030	0.020	0.034	0.158	0.572	0.999
Ruminococcaceae	0.071	0.074	0.046	0.024	0.037	0.025	0.554	0.999	0.276
S24-7	0.369	0.419	0.321	0.421	0.422	0.420	0.673	0.370	0.596
Unclassified‡	0.139	0.180	0.125	0.072	0.127	0.074	0.181	0.393	**0.040**
Other§	0.039	0.040	0.030	0.054	0.042	0.053	NA	NA	NA

Table 2b. Percent difference in relative abundance of families from time 0 to time 2 between control and treatment groups

	Time 0		**Time 1**		**Time 2**	
Family	**Difference (%)***	**T0 P-value†**	**Difference (%)***	**T1 P-value†**	**Difference (%)***	**T2 P-value†**
[Odoribacteraceae]	125.100	0.168	-37.586	0.139	-63.119	0.753
Bacteroidaceae	83.502	**0.027**	50.810	0.370	66.724	0.596
Bifidobacteriaceae	-13.211	0.673	-171.330	0.572	-107.564	0.276
Clostridiaceae	63.748	0.295	-155.555	0.393	-162.054	0.311
Defferribacteraceae	-123.079	0.519	-161.815	0.715	-173.080	0.958
Erysipelotrichaceae	123.071	0.673	-103.488	0.250	-73.827	0.592
F16	-63.345	0.377	-5.194	0.321	-63.171	0.223
Helicobacteraceae	-2.678	0.584	-69.601	0.265	-77.878	0.592
Lachnospiraceae	-68.697	**0.047**	46.000	0.600	22.429	0.276
Lactobacillaceae	-65.464	0.470	24.691	0.299	-18.243	0.592
Mycoplasmataceae	158.440	**0.045**	97.425	0.687	84.678	0.276
Porphyromonadaceae	132.594	**0.045**	5.567	0.606	72.026	0.383
Prevotellaceae	38.654	0.525	-4.823	0.687	10.489	0.912
Rikenellaceae	48.546	0.158	-19.193	0.572	-48.438	0.999
Ruminococcaceae	-4.430	0.554	64.093	0.999	38.503	0.276
S24-7	-12.818	0.673	-27.109	0.370	0.564	0.596

Unclassified‡	-25.805	0.181	53.194	0.393	53.548	**0.040**
Other§	-2.035	NA	-55.799	NA	-23.501	NA

*Positive values indicate a higher relative abundance in the control group and negative values indicate a higher relative abundance in the ACT group. Percent difference calculated as: (average relative abundance in controls – average relative abundance in ACT)/[(average relative abundance in controls + average relative abundance in ACT)/2]
†Bolded values indicate statistical significance ($p<0.05$). P-values were generated with unpaired Mann-Whitney U tests and adjusted using the Benjamini-Hochberg method.
‡"Unclassified" indicates that the OTU could not be matched at the level of 98% similarity to a bacterial family within the Ribosomal Data Project and Greengenes database.
§"Other' includes all families which constitute less than 1% of the average relative abundance per group.

Table 3a. Average relative abundance of genera from time 0 to time 2 between control and treatment groups

	Time 0		Time 1		Time 2				
Genus	**Control**	**ACT**	**Control**	**ACT**	**Control**	**ACT**	**T0 P-value†**	**T1 P-value†**	**T2 P-value†**
Allobaculum	0.015	0.000	0.007	0.014	0.076	0.022	0.721	0.198	0.190
Bacteroides	0.130	0.053	0.068	0.043	0.076	0.038	**0.005**	0.386	0.364
Bifidobacterium	0.002	0.002	0.002	0.028	0.005	0.016	0.333	0.182	0.332
Helicobacter	0.004	0.004	0.004	0.007	0.005	0.009	0.999	0.417	0.240
Lactobacillus	0.061	0.121	0.303	0.258	0.197	0.236	0.111	0.669	0.438
Mucispirillum	0.002	0.008	0.002	0.005	0.001	0.020	0.245	0.590	0.525
Odoribacter	0.039	0.009	0.008	0.012	0.006	0.012	**0.023**	0.161	0.332
Oscillospira	0.039	0.039	0.030	0.018	0.024	0.016	0.967	0.425	0.343
Parabacterides	0.031	0.006	0.007	0.008	0.011	0.005	**0.005**	0.536	0.231
Prevotella	0.018	0.018	0.024	0.021	0.021	0.022	0.556	0.910	0.606
Ureaplasma	0.014	0.002	0.001	0.000	0.001	0.000	**0.005**	0.226	0.139
Unclassified‡	0.605	0.695	0.516	0.542	0.610	0.565	**0.006**	0.585	0.566
Other§	0.047	0.061	0.052	0.064	0.062	0.045	NA	NA	NA

Table 3b. Percent difference in relative abundance of genera from time 0 to time 2 between control and treatment groups

	Time 0		Time 1		Time 2	
Genus	**Difference (%)***	**T0 P-value†**	**Difference (%)***	**T1 P-value†**	**Difference (%)***	**T2 P-value†**
Allobaculum	187.587	0.721	-70.867	0.198	108.663	0.190
Bacteroides	83.502	**0.005**	45.403	0.386	66.724	0.364
Bifidobacterium	-13.211	0.333	-175.725	0.182	-107.564	0.332
Helicobacter	-2.678	0.999	-62.723	0.417	-56.415	0.240
Lactobacillus	-65.464	0.111	15.922	0.669	-18.243	0.438
Mucispirillum	-123.079	0.245	-69.214	0.590	-173.080	0.525

Odoribacter	125.100	**0.023**	-47.376	0.161	-63.119	0.332
Oscillospira	-1.188	0.967	49.826	0.425	43.112	0.343
Parabacterides	132.594	**0.005**	-1.976	0.536	72.026	0.231
Prevotella	3.390	0.556	13.741	0.910	-7.424	0.606
Ureaplasma	158.440	**0.005**	85.028	0.226	84.678	0.139
Unclassified‡	-13.951	**0.006**	-4.839	0.585	7.809	0.566
Other§	-26.179	NA	-22.238	NA	30.348	NA

*Positive values indicate a higher relative abundance in the control group and negative values indicate a higher relative abundance in the ACT group. Percent difference calculated as: (average relative abundance in controls – average relative abundance in ACT)/[(average relative abundance in controls + average relative abundance in ACT)/2]

†Bolded values indicate statistical significance ($p<0.05$). P-values were generated with unpaired Mann-Whitney U tests and adjusted using the Benjamini-Hochberg method.

‡"Unclassified" indicates that the OTU could not be matched at the level of 98% similarity to a bacterial family within the Ribosomal Data Project and Greengenes database.

§"Other' includes all families which constitute less than 1% of the average relative abundance per group.

A. Dynamics between groups

We observed differences in the relative abundance of certain taxa at all timepoints. At baseline, the most notable differences between ACT and control groups were observed among some less prominent taxa including Deferribacteres (0.8 vs. 0.2%; p=0.229), Tenericutes (0.4 vs. 1.7%;; p=0.058), *Mycoplasmataceae* (0.2 vs. 1.4%; percent difference=158.4%; p=0.045), *Porphyromonadaceae* (0.6 vs. 3.1%; percent difference=132.6%; p=0.045), *Allobaculum* (0 vs. 1.5%; percent difference=187.6%; p=0.721), *Ureaplasma* (0.2 vs. 1.4%; percent difference=158.4%; p=0.005), and *Odoribacter* (0.9 vs. 3.9%; percent difference=125.1%; p=0.023) . (Tables 1a,2a,3a).

At time point 1 (6 weeks post-baseline), Actinobacteria were significantly more abundant in the ACT compared to the control group (3.3 vs. 0.5%; p=0.042). Families *Bifidobacteriaceae* (1.7 vs. 0.1%, percent difference=171.3%; p=0.572), *Defferribacteraceae* (1.8 vs. 0.2%, percent difference=161.8, p=0.715), and *Erysipelotrichaceae* (2.9 vs. 0.9%; percent difference=103.5%; p=0.250) and genus *Bifidobacterium* (2.8 vs. 0.2%; percent difference=175.7%; p=0.182) had higher relative abundance in the ACT group compared to the control group, though not reaching statistical significance (Tables 1a,2a,3a).

The differences in the average relative abundance of various taxa between the ACT and control groups at time point 2 (12 weeks post-baseline) followed a similar pattern to that observed at time point 1. More specifically, Deferribacteres (2.0 vs. 0.1%; p=0.898), Actinobacteria (2.0 vs. 0.8%; percent difference=90.7%; p=0.270), *Defferribacteraceae* (2.0 vs. 0.1%; percent difference=173.1%; p=0.958), *Bifidobacteriaceae* (1.6 vs. 0.5%; percent difference=107.6%; p=0.596), *Mucispirillum* (2.0 vs. 0.1%; difference=173.1%; p=0.245), and *Bifidobacterium* (1.6 vs. 0.5%; percent difference=107.6%; p=0.332) had higher average relative abundance in the ACT compared to the control group. Conversely, *Porphyromonadaceae* (0.5 vs. 1.1%; percent difference=72.0; p=0.383) and *Allobaculum* (2.2 vs. 7.6%; percent difference=108.7%; p=0.190) were less abundant in the ACT compared to the control group (Tables 1a,2a,3a).

B. Dynamics within groups

In the ACT group, the average relative abundance of taxa remained relatively stable over time. The most prominent changes from baseline to time point 1 were increases among Actinobacteria (0.5 vs. 3.3%; percent difference=148.7%; p=0.496), *Erysipelotrichaceae* (0.4 vs. 2.9% percent difference=151.4%; p=0.073), *Bifidobacteriaceae* (0.2 vs. 1.7%; percent difference=149.0%; p=0.082), *Allobaculum* (0 vs. 1.4%; percent difference=186.3%%; p=0.013), and *Bifidobacterium* (percent difference=167.1%; p=0.055) as well as decreases among *Ruminococcaceae* (7.4 vs. 2.4%; percent difference=103.1%; p=0.010) and *Oscillospira* (3.9 vs. 1.8%; percent difference=74.6%; p=0.015). The only notable changes observed from time point 1 to time point 2 were increases in Deferribacteres (0.4 vs. 2.0%; percent difference=126.6%; p=0.653) and *Mucispirillum* (0.5 vs. 2.0%; percent difference=120.9%; p=0.426). However, the relative abundance of many taxa changed, mostly observed as decreases, from time point 2 to time point 3 (27 weeks; 18 weeks post-baseline). Most prominently. the average relative abundance of Deferribacteres (2.0 vs. 0.2%; percent difference=159.2%; p=0.541), *Defferribacteraceae* (2.0 vs. 0.2%; percent difference=159.0; p=0.410), *Bifidobacteriadceae* (1.6 vs. 0.4%; percent difference=120.5%; p=0.106), *Mucispirillum* (percent difference=159.0; p=0.430), *Allobaculum* (2.2 vs. 0.6%; percent difference=120.25; p=0.078), and *Bifidobacterium* (1.6 vs. 0.4%; percent difference=120.5%; p=0.106) decreased from time point 2 to 3 (Tables 1b,2b,3b).

In the control group, the most prominent changes in the average relative abundance of taxa from baseline to time point 1 increases among Firmicutes (24.9 vs. 48.6%; percent difference=64.6%; p=0.63) and *Lactobacillus* (6.1 vs. 30.3%; percent difference=132.6%; p=0.094) and decreases among Tenericutes (1.7 vs. 0.6%; percent difference=90.7; p=0.313), *Mycoplasmataceae* (1.4 vs. 0.1%; percent difference=169.8; p=0.125), [*Odoribacteraceae*] (3.9 vs. 0.8%; percent difference=134.8%; p=0.125), *Ureaplasma* (1.4 vs. 0.1%; percent difference=169.8%; p=0.094) (Tables 1b,2b,3b), *Odoribacter* (3.9 vs. 0.8%; percent difference=134.8%; p=0.094), and *Parabacteroides* (3.1 vs. 0.7%; percent difference=123.9%; p=0.105). From time point 1 to time point 2, we observed notable increases in Proteobacteria (0.8 vs. 1.3%; percent difference=50.1%; p=0.167) and

Allobaculum (0.7 vs. 7.6%; percent difference=168.1; p=0.625) and a decrease in *Lactobacillaceae* (30.3 vs. 19.7%; percent difference=42.5%; p=0.375) (Tables 1b,2b,3b).

OTUs associated with ACT and control groups

The DESeq2 package within R was used to identify OTUs associated with treatment status at time points 1 and 2 through a differential abundance analysis[17]. A core microbiome (defined as all OTUs present in at least 70% of the samples per time point) associated with each time point was identified and used for these calculations. A total of 12 OTUs at time point 1 and 11 OTUs at time point 2 were identified as differentially abundant. The absolute value of the log2 fold changes ranged from 1.42 to 6.16 for time point 1 and 3.17 to 10.98 for time point 2. For time point 1, the OTUs observed to be increased in the ACT group were of the Bacteroidales order, *S24-7* family, and *Bifidobacterium*, *Desulfovibrio*, *Lactobacillus*, and *Odoribacter* genera. Those increased in the control group at time point 1 were of Clostridiales order, *Rikenellaceae* and *S24-7* families, and *Lactobacillus* genus. For time point 2, the OTUs increased in the ACT group were of Bacteroidales and RF39 orders, *Ruminococcaceae* and *S24-7* families, and *Aldercreutzia*, *Lactobacillus*, *Mucispirillum*, *Odoribacter*, and *Oscillospira* genera. Those increased in the control group at time point 2 were of the Clostridiales order and *Oscillospira* genus.

Figure 2. Plot of significantly differentially abundant bacterial taxa between ACT and control groups at time points 1 and 2

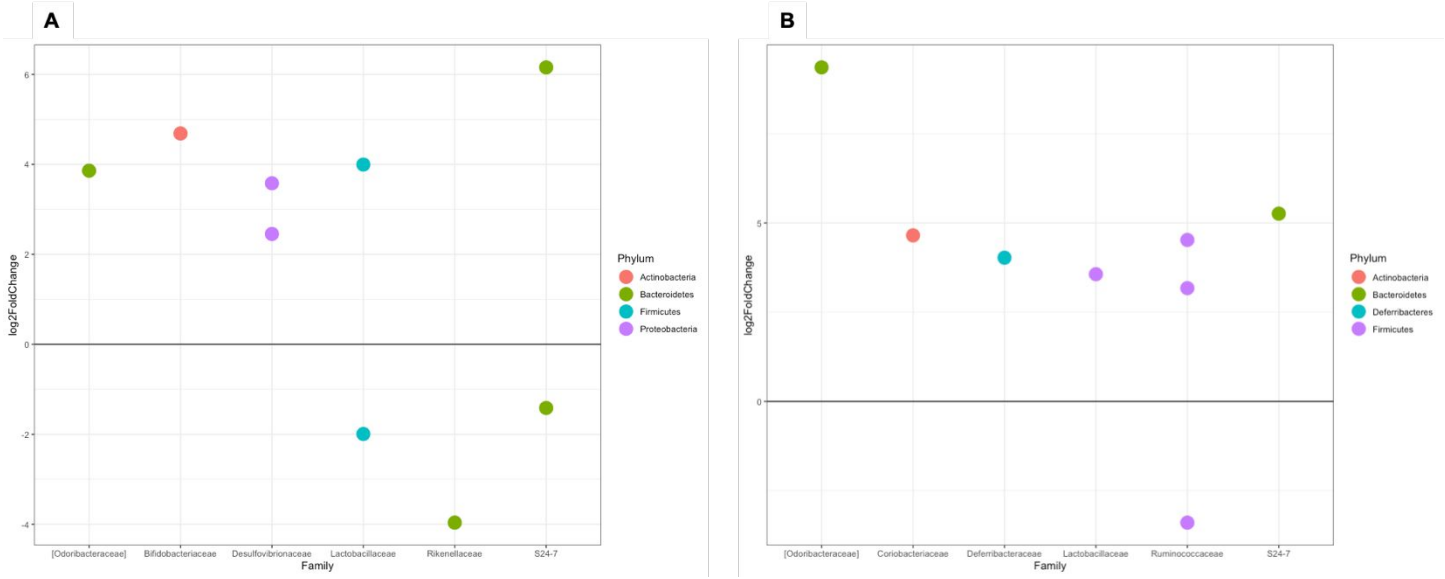

This graph depicts the magnitude of change (log2FoldChange) in terms of abundance between the ACT and control groups at (A) time point 1 and (B) time point 2. The black horizontal line indicates no change (R^2=0). All circles above this line represent OTUs more abundant in ACT group samples and all circles below this line represent OTUs more abundant in control group samples. The color of the circle indicates phylum and the location on the horizontal axis indicates family. All OTUs shown were found to be statistically significant (p<0.05) in terms of differential abundance using Wald's test with BH adjustment in the DESeq2 package (DESeq function). Data were normalized within the DESeq function for equitable comparison prior to analysis.

Trends in alpha diversity between groups and over time

Shannon diversity was not different between the ACT and control groups at baseline (4.55 vs. 4.24; p=0.133), time point 1 (4.16 vs. 4.01; p=0.601), or time point 2 (4.10 vs. 4.16; p=0.606). Similarly, Simpson's diversity was not different between the ACT and control groups at baseline (0.973 vs. 0.961; p=0.193), time point 1 (0.956 vs. 0.934; p=0.109), or time point 2 (0.957 vs. 0.959; p=0.297). However, some significant differences were identified within the ACT group over time. Shannon diversity significantly decreased from baseline to time point 1 (4.55 vs. 4.16; p=0.008) and significantly increased from time point 2 to time point 3 (4.10 vs. 4.490; p=0.020). Simpson's diversity followed a similar trend with differences identified from baseline to time point 1 (0.973 vs. 0.956; p=0.074) and time point 2 to time point 3 (p=0.039). No significant differences were observed between time points for either measure of alpha diversity within the control group.

Differences in community similarity between groups and over time

Unweighted UniFrac measures[18], representing similarity of microbiota composition and closeness of phylogenetic distance between samples, were plotted for each sample at each time point using a Principal Coordinates Analysis (PCoA) plot (Figure 2). Significant differences in the unweighted UniFrac measures were observed by group (ACT and controls) and time points 1 and 2 (R^2=0.221; p=0.002). Samples associated with time point 3 were not included in the statistical evaluation as they were exclusively from the ACT group (control mice did not survive to this time point). Clustering of samples can be observed at baseline and by group at each time point on the PCoA plot (Figure 3).

Figure 3. Clustering of samples by group (ACT vs. controls) over time using unweighted UniFrac measures

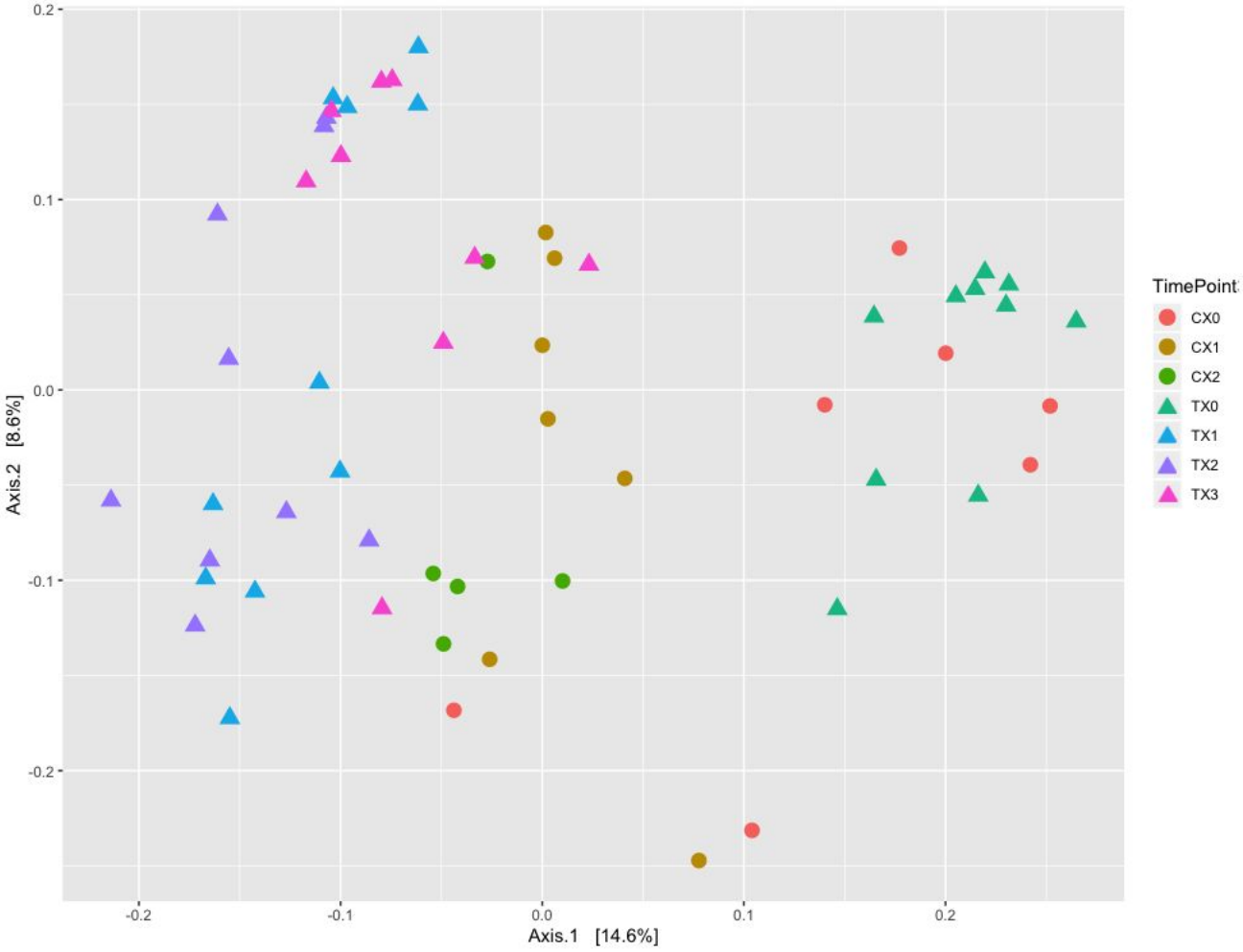

Clusters indicate similarity of microbiota composition and closeness in phylogenetic distance between samples measured by unweighted UniFrac distances. Each shape represents an individual sample. Colors indicate both time point and group. Circles indicate controls and triangles indicate treatment (ACT) mice. CX0 and TX0 indicate baseline and all subsequent numbers indicate the next corresponding time point (time point 1 = 6 weeks; time point 2 = 12 weeks; time point 3 = 18 weeks). Samples were determined to significantly cluster by group and time point (R^2=0.221; p=0.002) via PERMANOVA using the Adonis function in the R package vegan.

DISCUSSION

The stability of the core gut microbiome members over time observed in the ACT group, but not in the control (disease) group, suggests that treatment with ACT in the early stages of PD pathology may be capable of maintaining a normal microbiota composition and consequently preventing or minimizing dysbiosis. This may be possible through the early induction of a robust immune response to cells expressing mutant α-syn in the ENS, initiated by ACT. In addition to observing stability of core microbiota, we also observed an increase from baseline in the relative abundance of beneficial microbiota, such as *Bifidobacterium*. Similarly, an OTU of the *Bifidobacterium* genus was found to be associated with ACT injection after baseline. This finding is consistent

with a recent report that *Bifidobacterium* was observed to be negatively correlated with the progression of PD pathology over a two-year period[19]. *Bifidobacteria* are widely recognized as a probiotic and are capable of producing lactic acid[20], which is associated with homeostasis of the gut microbiota and modulation of immune response, as well as vitamin B9 (folate), which has been found to be neuroprotective in the context of various conditions including Alzheimer's disease[22]. We have previously shown that there are notable differences in metabolites in mice treated with immunotherapies when compared to controls[23], suggesting that shifts in gut microbiota can indeed affect metabolic pathways via the enteric nervous system (ENS).

Two OTUs of family *S24-7* and genus *Odoribacter* were also found to be associated with ACT post-baseline. Unfortunately, not much is currently known about the possible role of the Bacteroidales *S24-7* family as only three species have been cultured[24]. However, a recent study characterizing the genome of this family (genomes extracted from fecal samples from multiple hosts, including both humans and mice) found that some members may be capable of mechanisms related to protection against oxidative stress[25], which has been suggested to play a role in the clinical course of PD[26]. Species within the genus *Odoribacter* are capable of producing butyrate[27], a short-chain fatty acid (SCFA) which serves as a primary nutrient for intestinal epithelial cells and plays an important role in the regulation of gene expression, cell differentiation, immune modulation, and oxidative stress reduction in the gut[28]. Further, SCFAs are known to directly promote regulation of tight junction proteins of the gut epithelium and therefore maintain barrier integrity and prevent 'leaky gut'[29]. Maintenance of this barrier is thought to be protective of overall health status, as well as of PD specifically, as increased gut permeability has been shown to be associated with increased levels of inflammatory cytokines and deposition of α-syn in the ENS[30]. Interestingly, individuals with inflammatory bowel disease (IBD) have been found to have decreased relative abundance of *Odoribacter* species[31] as well as be at an increased risk for PD[32]. Conversely, Clostridiales order was found to be associated with the control (non-ACT) group at both times points post-baseline. Members of this order have been found to be selectively coated with IgA, a critical mediator of intestinal immunity, in patients with IBD compared to healthy controls[33]. These relationships suggests that gut inflammation, possibly partially due to reduced levels of SCFA-producing microbiota and increased levels of immunogenic microbiota, may be capable of initiating the early enteric stages of PD pathology (i.e. α-syn

release and aggregation as well as loss of dopaminergic neurons)[32]. ACT may represent a novel therapeutic intervention to diminish the influence of unfavorable microbiota composition on the underlying mechanisms of this early-stage pathology.

Similar to studies comparing the gut microbiome of individuals with and without PD [9], we did not observe any significant differences in alpha diversity between the ACT and control groups. However, we did detect statistically significant differences in unweighted UniFrac measures by both group and time point, suggesting distinct microbiota community dynamics associated with ACT treatment status. The changes in microbiota community composition observed in the control group over time were distinct and more pronounced than that of the ACT group. Therefore, an indirect benefit of ACT, apart from its function in initiating an immune response to target mutant α-syn, may be to minimize substantial shifts in gut microbiota that may lead to dysbiosis and exacerbation of PD. Our findings in a relevant PD mouse model suggest that microbiota dynamics might represent a promising target for improving efficacy of novel treatment approaches to slow PD progression. To expand upon our findings, studies in other PD models as well as in PD patients should include microbiota analyses to identify generalizable microbiota signatures associated with slowing of PD progression that can ultimately be utilized to improve treatment efficacy.

MATERIALS & METHODS

Animals

A total of 17 M83 heterozygous mice (transgenic mice overexpressing the human form of familial A53T mutant α-syn) were used in this study. Mice were divided into treatment (N=10) and control arms (N=7). Mice in the treatment arm were injected with a novel adoptive cellular therapy (ACT) intravenously at 8 weeks of age. Control mice were similarly injected with a saline solution at the same age. At 9 weeks (baseline), all mice received a peripheral injection of α-syn fibrils in the gastrocnemius muscle in order to induce CNS α-syn pathology. A single peripheral intramuscular injection of α-syn fibrils has previously been shown to induce α-syn aggregations and consequent motor impairment in transgenic mouse models of PD[12], and has been found to be more efficient in inducing robust CNS pathology compared to both intraperitoneal and tail vein injections[13]. Fecal pellets were

collected from all mice (treatment and control groups) at three time points: baseline, 6 weeks, and 12 weeks post injection. Fecal pellets were collected at an additional time point (18 weeks post injection) from all surviving mice (comprised of ACT group only). All experimental protocols were approved by institutional guidelines from the University of Florida Institutional Animal Care and Use Committee (20170838201).

16S Bacterial rDNA Extraction, Amplification, and Sequencing

16S bacterial rDNA was extracted from the fecal pellets using QIAmp PowerFecal DNA kit (Qiagen) following manufacturer protocols with the addition of a mechanical lysis bead-beating step (Biospec Products). Following extraction, DNA concentrations for each sample were measured using the Nanodrop platform to ensure adequate levels for amplification. DNA was then amplified via polymerase chain reaction (PCR) using barcoded primers for the V1-V2 hypervariable regions of the bacterial 16S rRNA genes. The concentration of barcoded PCR products for each sample were measured (Quati-iT dsDNA assay kit, Invitrogen) and equimolar amounts were then pooled and purified (Mag-Bind TotalPure NGS beads, Omega Bio Tek). The Illumina Mi-Seq platform was used to pair-end (250x2) sequence the samples.

Microbiota Data Processing

Quantitative Insights into Microbial Ecology 2 (QIIME2) tool (version 2019.7; open source software)[34] pipeline was used to trim and quality filter sequences. Amplicon Sequence Variants (ASVs) were determined using Deblur[35], and clustered into de novo operational taxonomic units (OTUs) at the 98% similarity level using VSEARCH[36]. Rarefaction curves to assess species richness and comparability of the samples were also generated through these pipelines. Chimeras were removed and taxonomy was assigned to OTUs using a classifier built with Scikit-learn[37] and verified against the Greengenes 16S rRNA gene database[38]. A phylogenetic tree for diversity analyses was generated with the FastTree pipeline[39]. Normalization, a procedure used to render all samples comparable by removing bias due to variable sequencing depths, was performed prior to conducting ordination or differential abundance analyses. The procedure chosen for this analysis involves the log transformation of OTU counts using the formula suggested by McCurdie and Holmes[40], log(1+x), which accounts for the high proportion of zero counts naturally present in microbiome datasets. Beta diversity (community diversity between samples) was assessed using unweighted UniFrac measures of phylogenetic distance generated

by Phyloseq[40]. Alpha diversity (diversity within a sample) was assessed using Shannon Diversity calculated with Phyloseq[40]. DESEq2[41] was used to conduct differential abundance analyses.

Statistical Analysis

Mann-Whitney Wilcoxon and Wilcoxon Signed Rank tests were used to assess differences in the relative abundance of taxa between and within groups at various time points, respectively. Mann-Whitney Wilcoxon test was also used to assess differences in alpha diversity measures between groups at each time point. Permutational Multivariate Analysis of Variance Using Distance Matrices (PERMANOVA) with 99 permutations was performed, using the Adonis function in the R package vegan[42], to evaluate the differences in unweighted UniFrac[18] distance measures between groups over time. Wald's test, run within the DESeq function, was used to identify OTUs that were significantly differentially abundant OTUs between groups at each time point. P-values generated for differences in relative abundance and differential abundance were adjusted for multiple comparisons using the Benjamini-Hochberg approach. A p-value of less than 0.05 was considered statistically significant.

Author's roles:
Emily Klann: Design and execution of statistical analysis; Manuscript preparation
Massimiliano Tagliamonte: Design and execution of statistical analysis; Review and critique of statistical analysis; Review and critique of manuscript
Maria Ukhanova: Execution of project related to DNA extraction and sequencing; Review and critique of manuscript
*Volker Mai: Project conception and organization; Review and critique of statistical analysis; Review and critique of manuscript
*Vinata Vedam-Mai: Project conception, organization, and execution; Review and critique of statistical analysis; Review and critique of manuscript

ORCiDs:
Emily Klann: 0000-0001-8930-4729
Massimiliano S. Tagliamonte: 0000-0003-2699-7331
Maria Ukhanova: 0000-0003-1223-9273
*Vinata Vedam-Mai: 0000-0003-0148-3297
*Volker Mai: 0000-0002-6997-9750

Corresponding author information:
- **Name:** Vinata Vedam-Mai, PhD
- **Address:** 1149 S. Newell Drive, L3-183, McKnight Brain Institute, University of Florida, Gainesville, FL, 32611
- **Phone number:** (352) 273-5557
- **Fax number:** (352) 273-5575
- **Email address:** vinved@neurology.ufl.edu

Conflicts of interest and financial disclosures: Vinata Vedam-Mai is supported by NINDS, the Mangurian Foundation, UF Foundation, and Abbott funds. Volker Mai, Massimiliano S. Tagliamonte, Maria Ukhanova, and Emily Klann declare no financial or any other conflicts of interest to disclose.

Study funding: This study was supported by funds from NINDS Grant (1R56NS112401-01), the Mangurian Foundation, and UF Foundation funds.

Ethical statement: All experimental protocols were approved by institutional guidelines from the University of Florida Institutional Animal Care and Use Committee (20170838201).

***These authors contributed equally and are co-senior authors.**

REFERENCES

(1) Nussbaum, R. L. Alzheimer's Disease and Parkinson's Disease. *N. Engl. J. Med.* **2003**, *348* (14), 1356–1364.

(2) Samii, A.; Nutt, J. G.; Ransom, B. R. Parkinson's Disease. *The Lancet* **2004**, *363* (9423), 1783–1793. https://doi.org/10.1016/S0140-6736(04)16305-8.

(3) Scheperjans, F.; Derkinderen, P.; Borghammer, P. The Gut and Parkinson's Disease: Hype or Hope? *J. Park. Dis. 8* (Suppl 1), S31–S39. https://doi.org/10.3233/JPD-181477.

(4) Tibar, H.; El Bayad, K.; Bouhouche, A.; Ait Ben Haddou, E. H.; Benomar, A.; Yahyaoui, M.; Benazzouz, A.; Regragui, W. Non-Motor Symptoms of Parkinson's Disease and Their Impact on Quality of Life in a Cohort of Moroccan Patients. *Front. Neurol.* **2018**, *9*, 170. https://doi.org/10.3389/fneur.2018.00170.

(5) Scheperjans, F.; Aho, V.; Pereira, P. A. B.; Koskinen, K.; Paulin, L.; Pekkonen, E.; Haapaniemi, E.; Kaakkola, S.; Eerola-Rautio, J.; Pohja, M.; Kinnunen, E.; Murros, K.; Auvinen, P. Gut Microbiota Are Related to Parkinson's Disease and Clinical Phenotype. *Mov. Disord.* **2015**, *30* (3), 350–358. https://doi.org/10.1002/mds.26069.

(6) Keshavarzian, A.; Green, S. J.; Engen, P. A.; Voigt, R. M.; Naqib, A.; Forsyth, C. B.; Mutlu, E.; Shannon, K. M. Colonic Bacterial Composition in Parkinson's Disease. *Mov. Disord.* **2015**, *30* (10), 1351–1360. https://doi.org/10.1002/mds.26307.

(7) Unger, M. M.; Spiegel, J.; Dillmann, K.-U.; Grundmann, D.; Philippeit, H.; Bürmann, J.; Faßbender, K.; Schwiertz, A.; Schäfer, K.-H. Short Chain Fatty Acids and Gut Microbiota Differ between Patients with Parkinson's Disease and Age-Matched Controls. *Parkinsonism Relat. Disord.* **2016**, *32*, 66–72. https://doi.org/10.1016/j.parkreldis.2016.08.019.

(8) Dutta, S. K.; Verma, S.; Jain, V.; Surapaneni, B. K.; Vinayek, R.; Phillips, L.; Nair, P. P. Parkinson's Disease: The Emerging Role of Gut Dysbiosis, Antibiotics, Probiotics, and Fecal Microbiota Transplantation. *J. Neurogastroenterol. Motil.* **2019**, *25* (3), 363–376. https://doi.org/10.5056/jnm19044.

(9) Haikal, C.; Chen, Q.-Q.; Li, J.-Y. Microbiome Changes: An Indicator of Parkinson's Disease? *Transl. Neurodegener.* **2019**, *8* (1), 38. https://doi.org/10.1186/s40035-019-0175-7.

(10) Tamtaji, O. R.; Taghizadeh, M.; Kakhaki, R. D.; Kouchaki, E.; Bahmani, F.; Borzabadi, S.; Oryan, S.; Mafi, A.; Asemi, Z. Clinical and Metabolic Response to Probiotic Administration in People with Parkinson's Disease: A Randomized, Double-Blind, Placebo-Controlled Trial. *Clin. Nutr.* **2019**, *38* (3), 1031–1035. https://doi.org/10.1016/j.clnu.2018.05.018.

(11) Bridi, J. C.; Hirth, F. Mechanisms of α-Synuclein Induced Synaptopathy in Parkinson's Disease. *Front. Neurosci.* **2018**, *12,* 80. https://doi.org/10.3389/fnins.2018.00080.

(12) Sacino, A. N.; Brooks, M.; Thomas, M. A.; McKinney, A. B.; Lee, S.; Regenhardt, R. W.; McGarvey, N. H.; Ayers, J. I.; Notterpek, L.; Borchelt, D. R.; Golde, T. E.; Giasson, B. I. Intramuscular Injection of α-Synuclein Induces CNS α-Synuclein Pathology and a Rapid-Onset Motor Phenotype in Transgenic Mice. *Proc. Natl. Acad. Sci. U. S. A.* **2014**, *111* (29), 10732–10737. https://doi.org/10.1073/pnas.1321785111.

(13) Ayers, J. I.; Brooks, M. M.; Rutherford, N. J.; Howard, J. K.; Sorrentino, Z. A.; Riffe, C. J.; Giasson, B. I. Robust Central Nervous System Pathology in Transgenic Mice Following Peripheral Injection of α-Synuclein Fibrils. *J. Virol.* **2017**, *91* (2), e02095-16. https://doi.org/10.1128/JVI.02095-16.

(14) Caggiu, E.; Arru, G.; Hosseini, S.; Niegowska, M.; Sechi, G.; Zarbo, I. R.; Sechi, L. A. Inflammation, Infectious Triggers, and Parkinson's Disease. *Front. Neurol.* **2019**, *10*, 122. https://doi.org/10.3389/fneur.2019.00122.

(15) Ngkelo, A.; Meja, K.; Yeadon, M.; Adcock, I.; Kirkham, P. A. LPS Induced Inflammatory Responses in Human Peripheral Blood Mononuclear Cells Is Mediated through NOX4 and Giα Dependent PI-3kinase Signalling. *J. Inflamm.* **2012**, *9* (1), 1. https://doi.org/10.1186/1476-9255-9-1.

(16) Ferrari, C. C.; Tarelli, R. Parkinson's Disease and Systemic Inflammation. *Park. Dis.* **2011**, *2011*, 436813. https://doi.org/10.4061/2011/436813.

(17) Love, M. I.; Huber, W.; Anders, S. Moderated Estimation of Fold Change and Dispersion for RNA-Seq Data with DESeq2. *Genome Biol.* **2014**, *15* (12), 550. https://doi.org/10.1186/s13059-014-0550-8.
(18) Lozupone, C.; Lladser, M. E.; Knights, D.; Stombaugh, J.; Knight, R. UniFrac: An Effective Distance Metric for Microbial Community Comparison. *ISME J.* **2011**, *5* (2), 169–172. https://doi.org/10.1038/ismej.2010.133.
(19) Minato, T.; Maeda, T.; Fujisawa, Y.; Tsuji, H.; Nomoto, K.; Ohno, K.; Hirayama, M. Progression of Parkinson's Disease Is Associated with Gut Dysbiosis: Two-Year Follow-up Study. *PLoS ONE* **2017**, *12* (11), e0187307. https://doi.org/10.1371/journal.pone.0187307.
(20) Ventura, M.; Turroni, F.; Lugli, G. A.; Sinderen, D. van. Bifidobacteria and Humans: Our Special Friends, from Ecological to Genomics Perspectives. *J. Sci. Food Agric.* **2014**, *94* (2), 163–168. https://doi.org/10.1002/jsfa.6356.
(21) Pompei, A.; Cordisco, L.; Amaretti, A.; Zanoni, S.; Matteuzzi, D.; Rossi, M. Folate Production by Bifidobacteria as a Potential Probiotic Property. *Appl. Environ. Microbiol.* **2007**, *73* (1), 179–185. https://doi.org/10.1128/AEM.01763-06.
(22) Dhiman, M.; Singh, G. Possible Neuroprotective Effects of Caveolin 1 Inhibitor, Curcumin with Association of Folic Acid and Vitamin B12 on ICV STZ Induced Alzheimer Disease in Rats. *J. Neurol. Sci.* **2019**, *405*, 99–100. https://doi.org/10.1016/j.jns.2019.10.958.
(23) Gill, E. L.; Koelmel, J. P.; Meke, L.; Yost, R. A.; Garrett, T. J.; Okun, M. S.; Flores, C.; Vedam-Mai, V. Ultrahigh-Performance Liquid Chromatography-High-Resolution Mass Spectrometry Metabolomics and Lipidomics Study of Stool from Transgenic Parkinson's Disease Mice Following Immunotherapy. *J. Proteome Res.* **2020**, *19* (1), 424–431. https://doi.org/10.1021/acs.jproteome.9b00605.
(24) Lagkouvardos, I.; Lesker, T. R.; Hitch, T. C. A.; Gálvez, E. J. C.; Smit, N.; Neuhaus, K.; Wang, J.; Baines, J. F.; Abt, B.; Stecher, B.; Overmann, J.; Strowig, T.; Clavel, T. Sequence and Cultivation Study of Muribaculaceae Reveals Novel Species, Host Preference, and Functional Potential of This yet Undescribed Family. *Microbiome* **2019**, *7* (1), 28. https://doi.org/10.1186/s40168-019-0637-2.
(25) Osaka, T.; Moriyama, E.; Arai, S.; Date, Y.; Yagi, J.; Kikuchi, J.; Tsuneda, S. Meta-Analysis of Fecal Microbiota and Metabolites in Experimental Colitic Mice during the Inflammatory and Healing Phases. *Nutrients* **2017**, *9* (12), 1329. https://doi.org/10.3390/nu9121329.
(26) Wei, Z.; Li, X.; Li, X.; Liu, Q.; Cheng, Y. Oxidative Stress in Parkinson's Disease: A Systematic Review and Meta-Analysis. *Front. Mol. Neurosci.* **2018**, *11,* 236. https://doi.org/10.3389/fnmol.2018.00236.
(27) Anand, S.; Kaur, H.; Mande, S. S. Comparative In Silico Analysis of Butyrate Production Pathways in Gut Commensals and Pathogens. *Front. Microbiol.* **2016**, *7,* 1945. https://doi.org/10.3389/fmicb.2016.01945.
(28) Bedford, A.; Gong, J. Implications of Butyrate and Its Derivatives for Gut Health and Animal Production. *Anim. Nutr.* **2018**, *4* (2), 151–159. https://doi.org/10.1016/j.aninu.2017.08.010.
(29) Morrison, D. J.; Preston, T. Formation of Short Chain Fatty Acids by the Gut Microbiota and Their Impact on Human Metabolism. *Gut Microbes* **2016**, *7* (3), 189–200. https://doi.org/10.1080/19490976.2015.1134082.
(30) Yang, D.; Zhao, D.; Ali Shah, S. Z.; Wu, W.; Lai, M.; Zhang, X.; Li, J.; Guan, Z.; Zhao, H.; Li, W.; Gao, H.; Zhou, X.; Yang, L. The Role of the Gut Microbiota in the Pathogenesis of Parkinson's Disease. *Front. Neurol.* **2019**, *10,* 1155. https://doi.org/10.3389/fneur.2019.01155.
(31) Morgan, X. C.; Tickle, T. L.; Sokol, H.; Gevers, D.; Devaney, K. L.; Ward, D. V.; Reyes, J. A.; Shah, S. A.; LeLeiko, N.; Snapper, S. B.; Bousvaros, A.; Korzenik, J.; Sands, B. E.; Xavier, R. J.; Huttenhower, C. Dysfunction of the Intestinal Microbiome in Inflammatory Bowel Disease and Treatment. *Genome Biol.* **2012**, *13* (9), R79. https://doi.org/10.1186/gb-2012-13-9-r79.
(32) Brudek, T. Inflammatory Bowel Diseases and Parkinson's Disease. *J. Park. Dis. 9* (Suppl 2), S331–S344. https://doi.org/10.3233/JPD-191729.
(33) Palm, N. W.; de Zoete, M. R.; Cullen, T. W.; Barry, N. A.; Stefanowski, J.; Hao, L.; Degnan, P. H.; Hu, J.; Peter, I.; Zhang, W.; Ruggiero, E.; Cho, J. H.; Goodman, A. L.; Flavell, R. A. Immunoglobulin A Coating

Identifies Colitogenic Bacteria in Inflammatory Bowel Disease. *Cell* **2014**, *158* (5), 1000–1010. https://doi.org/10.1016/j.cell.2014.08.006.

(34) Bolyen, E.; Rideout, J. R.; Dillon, M. R.; Bokulich, N. A.; Abnet, C. C.; Al-Ghalith, G. A.; Alexander, H.; Alm, E. J.; Arumugam, M.; Asnicar, F.; Bai, Y.; Bisanz, J. E.; Bittinger, K.; Brejnrod, A.; Brislawn, C. J.; Brown, C. T.; Callahan, B. J.; Caraballo-Rodríguez, A. M.; Chase, J.; Cope, E. K.; Da Silva, R.; Diener, C.; Dorrestein, P. C.; Douglas, G. M.; Durall, D. M.; Duvallet, C.; Edwardson, C. F.; Ernst, M.; Estaki, M.; Fouquier, J.; Gauglitz, J. M.; Gibbons, S. M.; Gibson, D. L.; Gonzalez, A.; Gorlick, K.; Guo, J.; Hillmann, B.; Holmes, S.; Holste, H.; Huttenhower, C.; Huttley, G. A.; Janssen, S.; Jarmusch, A. K.; Jiang, L.; Kaehler, B. D.; Kang, K. B.; Keefe, C. R.; Keim, P.; Kelley, S. T.; Knights, D.; Koester, I.; Kosciolek, T.; Kreps, J.; Langille, M. G. I.; Lee, J.; Ley, R.; Liu, Y.-X.; Loftfield, E.; Lozupone, C.; Maher, M.; Marotz, C.; Martin, B. D.; McDonald, D.; McIver, L. J.; Melnik, A. V.; Metcalf, J. L.; Morgan, S. C.; Morton, J. T.; Naimey, A. T.; Navas-Molina, J. A.; Nothias, L. F.; Orchanian, S. B.; Pearson, T.; Peoples, S. L.; Petras, D.; Preuss, M. L.; Pruesse, E.; Rasmussen, L. B.; Rivers, A.; Robeson, M. S.; Rosenthal, P.; Segata, N.; Shaffer, M.; Shiffer, A.; Sinha, R.; Song, S. J.; Spear, J. R.; Swafford, A. D.; Thompson, L. R.; Torres, P. J.; Trinh, P.; Tripathi, A.; Turnbaugh, P. J.; Ul-Hasan, S.; van der Hooft, J. J. J.; Vargas, F.; Vázquez-Baeza, Y.; Vogtmann, E.; von Hippel, M.; Walters, W.; Wan, Y.; Wang, M.; Warren, J.; Weber, K. C.; Williamson, C. H. D.; Willis, A. D.; Xu, Z. Z.; Zaneveld, J. R.; Zhang, Y.; Zhu, Q.; Knight, R.; Caporaso, J. G. Reproducible, Interactive, Scalable and Extensible Microbiome Data Science Using QIIME 2. *Nat. Biotechnol.* **2019**, *37* (8), 852–857. https://doi.org/10.1038/s41587-019-0209-9.

(35) Amir, A.; McDonald, D.; Navas-Molina, J. A.; Kopylova, E.; Morton, J. T.; Zech Xu, Z.; Kightley, E. P.; Thompson, L. R.; Hyde, E. R.; Gonzalez, A.; Knight, R. Deblur Rapidly Resolves Single-Nucleotide Community Sequence Patterns. *mSystems* **2017**, *2* (2), e00191-16. https://doi.org/10.1128/mSystems.00191-16.

(36) Rognes, T.; Flouri, T.; Nichols, B.; Quince, C.; Mahé, F. VSEARCH: A Versatile Open Source Tool for Metagenomics. *PeerJ* **2016**, *4*, e2584. https://doi.org/10.7717/peerj.2584.

(37) Pedregosa, F.; Varoquaux, G.; Gramfort, A.; Michel, V.; Thirion, B.; Grisel, O.; Blondel, M.; Prettenhofer, P.; Weiss, R.; Dubourg, V.; Vanderplas, J.; Passos, A.; Cournapeau, D.; Brucher, M.; Perrot, M.; Duchesnay, É. Scikit-Learn: Machine Learning in Python. *J. Mach. Learn. Res.* **2011**, *12* (85), 2825–2830.

(38) DeSantis, T. Z.; Hugenholtz, P.; Larsen, N.; Rojas, M.; Brodie, E. L.; Keller, K.; Huber, T.; Dalevi, D.; Hu, P.; Andersen, G. L. Greengenes, a Chimera-Checked 16S RRNA Gene Database and Workbench Compatible with ARB. *Appl Env. Microbiol* **2006**, *72* (7), 5069–5072. https://doi.org/10.1128/AEM.03006-05.

(39) Price, M. N.; Dehal, P. S.; Arkin, A. P. FastTree 2 – Approximately Maximum-Likelihood Trees for Large Alignments. *PLOS ONE* **2010**, *5* (3), e9490. https://doi.org/10.1371/journal.pone.0009490.

(40) McMurdie, P. J.; Holmes, S. Phyloseq: An R Package for Reproducible Interactive Analysis and Graphics of Microbiome Census Data. *PLOS ONE* **2013**, *8* (4), e61217. https://doi.org/10.1371/journal.pone.0061217.

(41) Love, M. I.; Huber, W.; Anders, S. Moderated Estimation of Fold Change and Dispersion for RNA-Seq Data with DESeq2. *Genome Biol.* **2014**, *15* (12), 550. https://doi.org/10.1186/s13059-014-0550-8.

(42) Jari Oksanen; F. Guillaume, B.; Friendly, M.; Roeland Kindt; Pierre Legendre; Dan McGlinn; Peter R. Minchin; R. B. O'Hara; Gavin L. Simpson; Peter Solymos; M. Henry H. Stevens; Eduard Szoecs; Helene Wagner. *Vegan: Community Ecology Package. R Package*; 2019.

For Table of Contents Only